

Supporting Information (SI) for

Multi-step electrodeposited hierarchical Ni-Co-P@LDHs nanocomposites for high-performance interdigital asymmetric micro- supercapacitors

Jianhui Zhan^a, Hui Yang^{a,b}, Qilong Zhang^{a,b,*}, Quan Zong^a, Wei Du^a, Qianqian Wang^a.

a School of Materials Science and Engineering, State Key Lab Silicon Mat, Zhejiang University, Hangzhou 310027, PR China

b ZJU-Guangxi-ASEAN Innovation & Research Center, Nanning 530022, PR China

**Corresponding Author. E-mail: mse237@zju.edu.cn*

1. synthesis of FeOOH on interdigital Au/PET substrate

The synthesis process of FeOOH, the anode material, is also via an electrodeposition step. Firstly, 0.86 g CH₃COONa and 0.98 g (NH₄)₂Fe(SO₄)₂ were added into 245 mL DI, 5 mL 1 M H₂SO₄ solution was also added for inhibiting the hydrolysis of Fe²⁺. After stirring, excess reduced iron powder was added into the solution to adjust the pH. Then the depositing process was carried out via a standard three-electrode system, in which one finger of conductive Au/PET substrate was employed as the working electrode. FeOOH nanosheets were electrodeposited via potentiostatic method, under the potential of 0.8 V (vs. SCE) at 65°C for 100 min. After deposition, the Au/PET substrate was slightly rinsed by DI and ethanol for three times respectively, then it was transferred into a vacuum oven and dried at 60 °C for 4 h.

2. preparation of PVA-KOH gel

PVA/KOH gel was prepared as the following method: 2.0 g PVA-1788 was firstly dissolved into 20 mL DI and kept stirring at low speed under 80 °C for 2 h. Then, a solution contains 1.68 g KOH and 10 mL DI was dropwise added into the transparent polymer solution under stirring. At last, the PVA/KOH gel was prepared after cooling and low-speed stirring at room temperature.

3. The low-scan rate CV curves of Ni-Co-P electrode and LDHs electrode

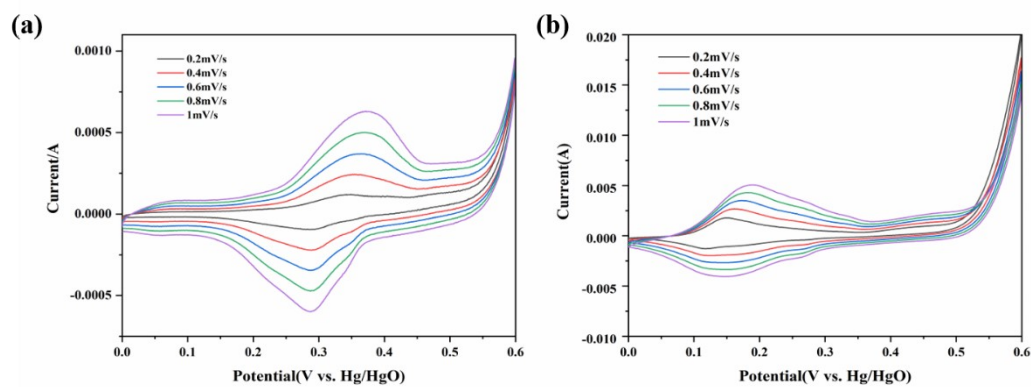


Fig S1. CV curves of (a) Ni-Co-P electrode, (b) LDHs electrode at low scan rates from 0.2 to 1 mV

s⁻¹.

4. The *i-t* and CV curves of electrodepositing process

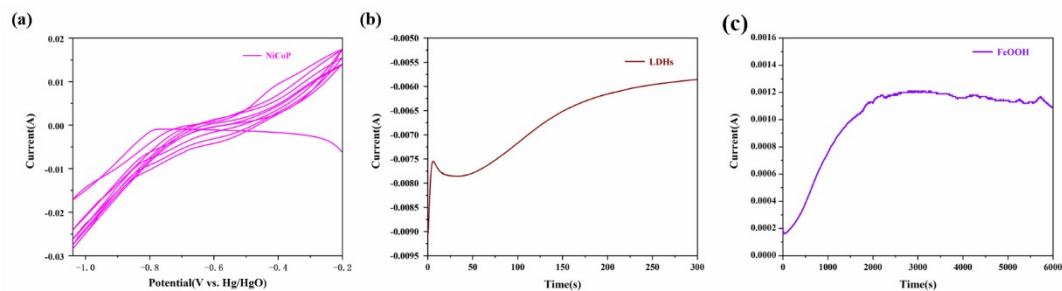


Fig S2. (a) CV curves of Ni-Co-P electrodeposition; (b) *i-t* curves of LDHs electrodeposition; (c) *i-t* curves of FeOOH electrodeposition.

5. The electrochemical performance of individual FeOOH electrode

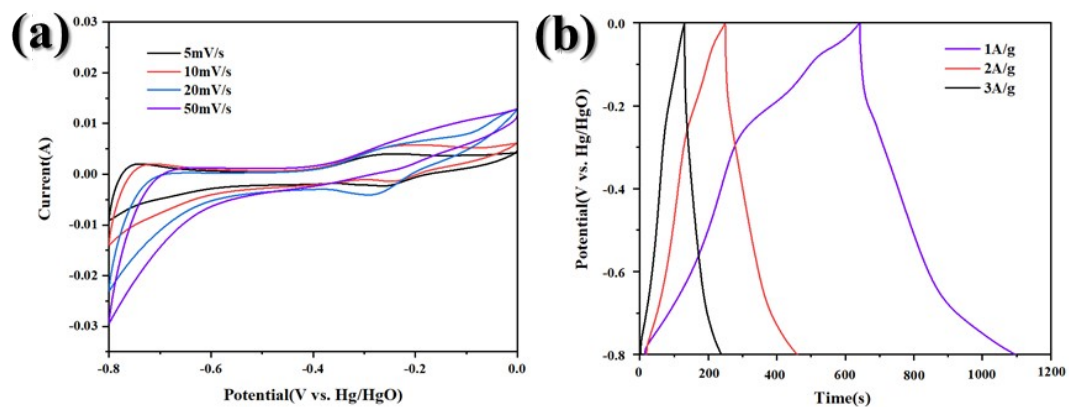


Fig S3. (a) CV curves at different scan rates, (b) GCD curves at different current density of individual FeOOH electrode.

6. The macro and micro appearances of AMSC Ni-Co-P//PVA-KOH//FeOOH

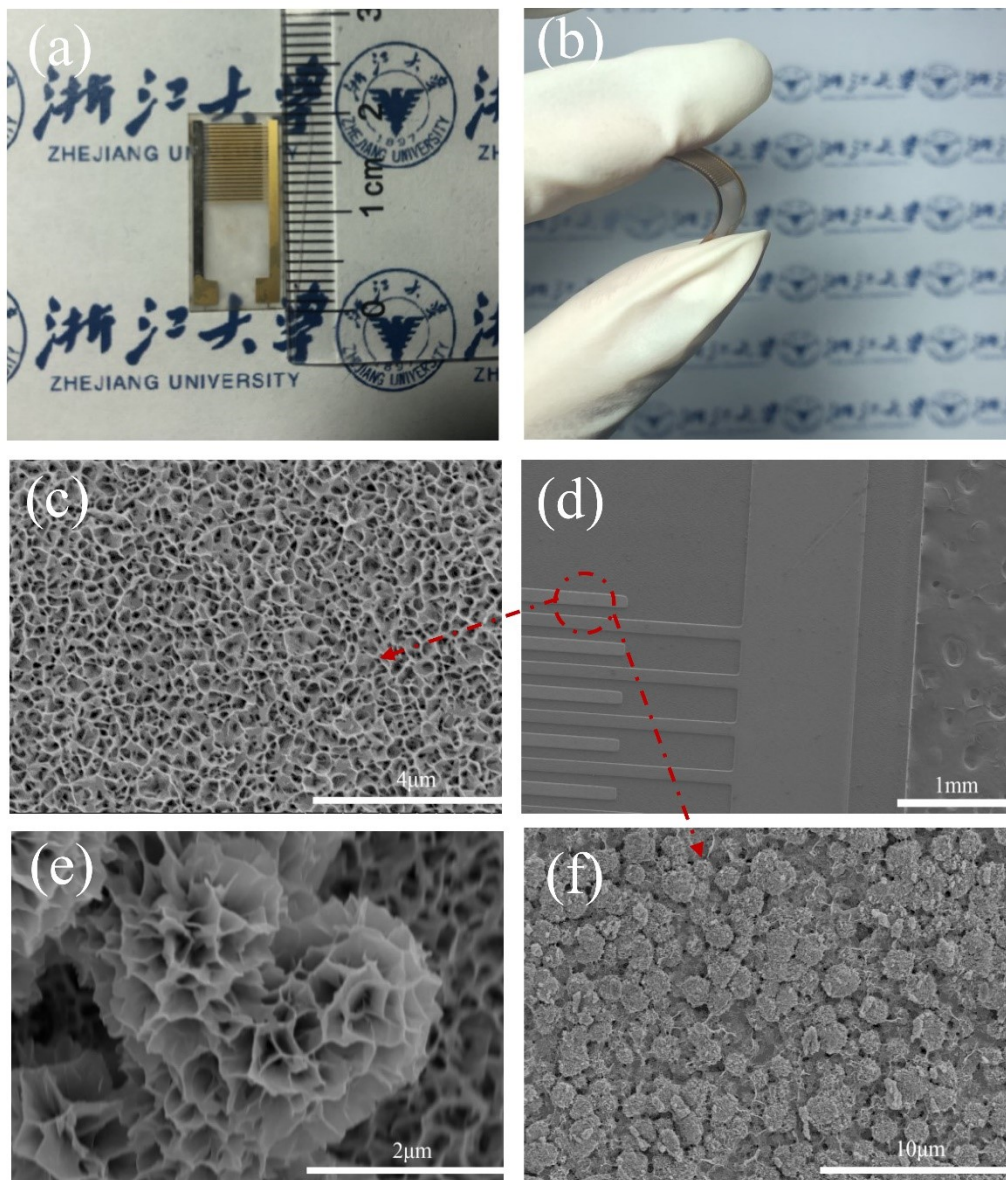


Fig S4. (a) The macro appearance and (b) The flexibility of as-prepared interdigital electrodes; (c) The SEM images of FeOOH nanosheets deposited on the Au finger; (d) The SEM images of the interdigital substrate; (e) A heart-shaped nanoflower of FeOOH; (f) The SEM images of Ni-Co-P@LDHs nanocomposites deposited on the Au finger

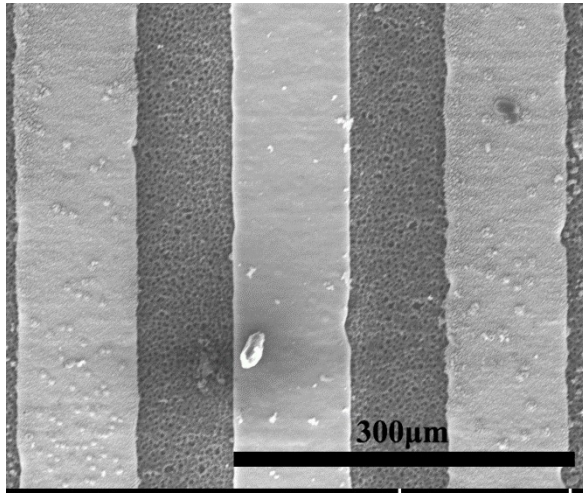


Fig S5. The SEM image of AMSC device.

7. The characterization of FeOOH

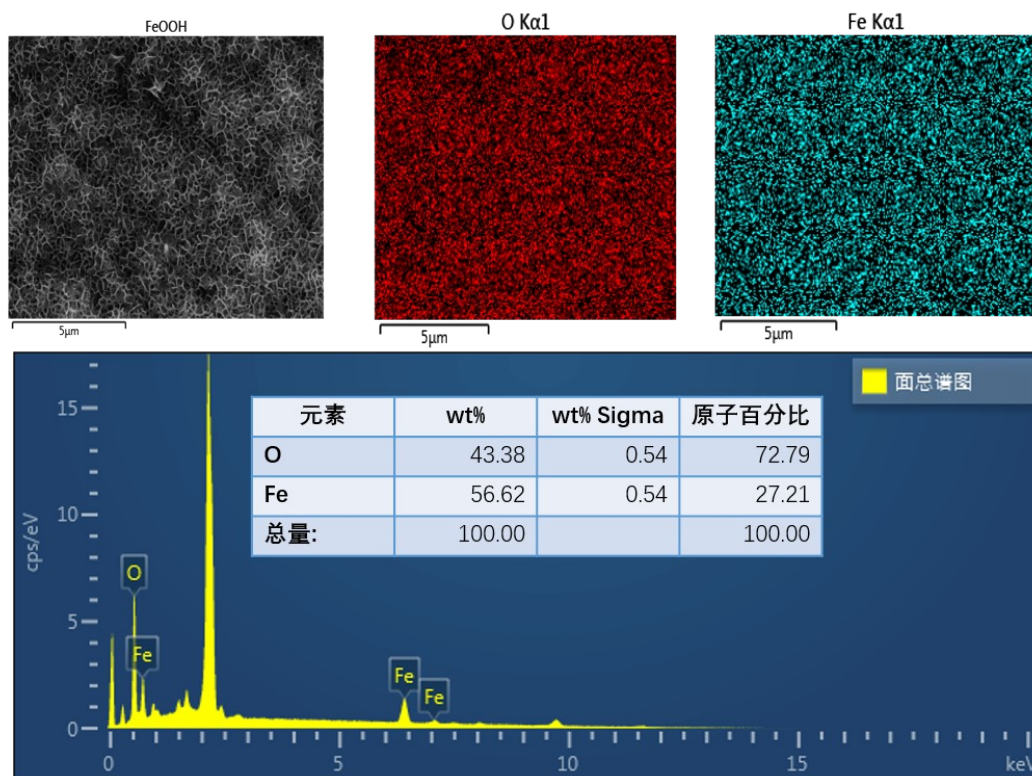


Fig S6. The EDS mapping images of FeOOH nanosheets.

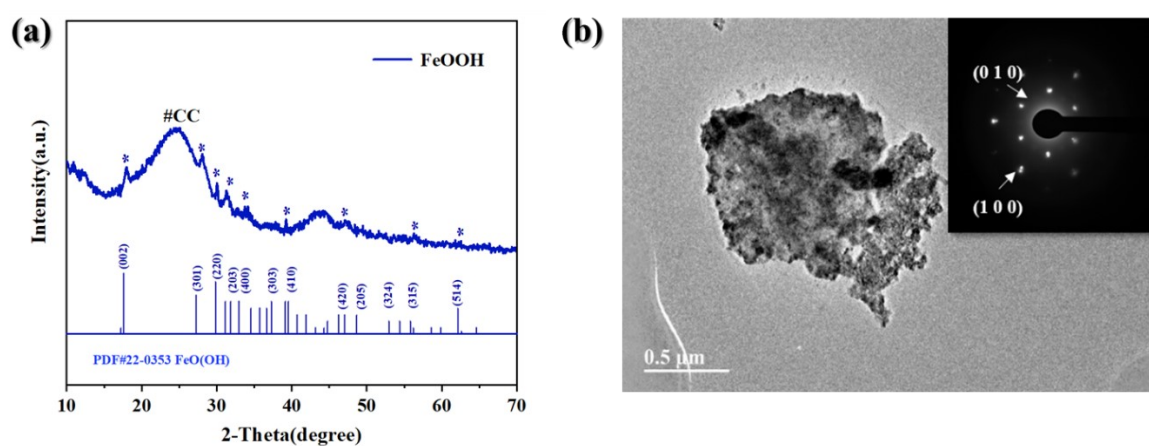


Fig S7. (a) The XRD pattern, (b) The TEM image and SAED pattern of FeOOH nanosheets.

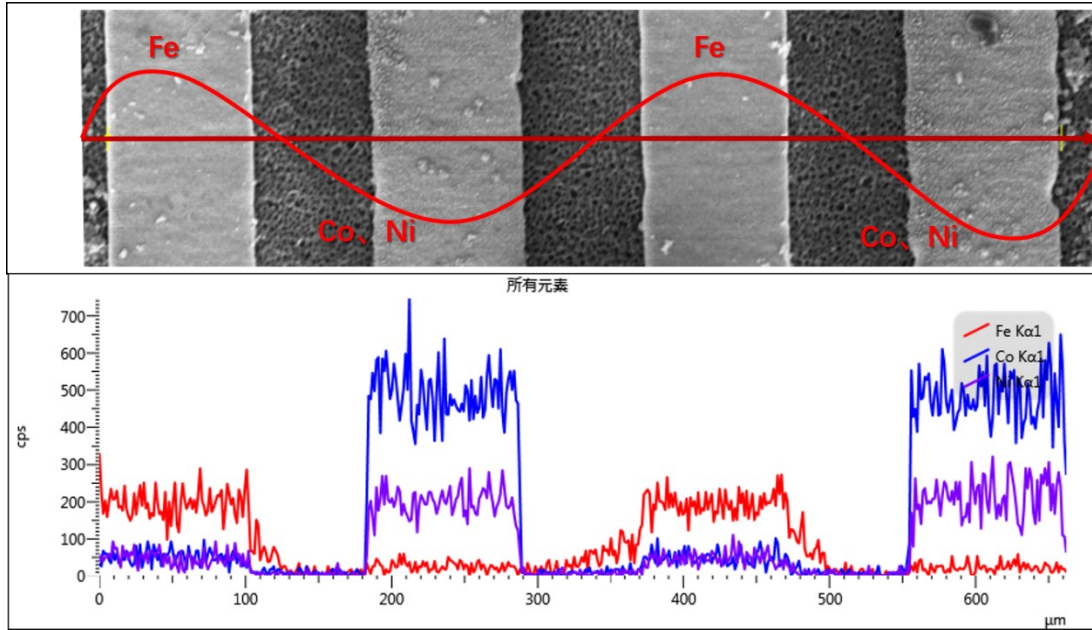


Fig S8. The EDS distribution of Fe, Co and Ni along the direction perpendicular to the fingers.

8. The equivalent circuit in fitting

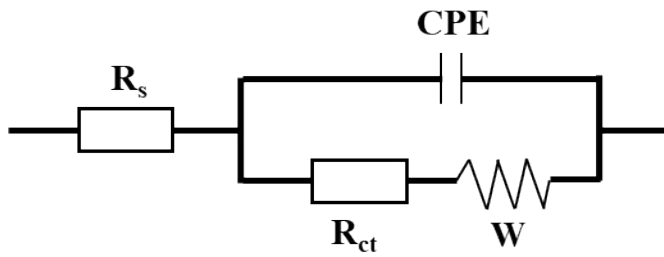


Fig S9. The equivalent circuit in EIS tests and fitting processes.

Table S1

Comparison on the working voltage and areal capacitance of different interdigital micro-supercapacitors.

Positive materials	Negative materials	Electrolyte	Working voltage	Areal capacitance	Refs.
ZIF-8 derived carbon	ZIF-8 derived carbon	PVA/KOH	0.8 V	—	1
MXene	RGO	PVA/H ₂ SO ₄	1.0 V	2.4 mF cm ⁻²	2
MnO ₂	Ag	PVA/KOH	1.0 V	46.6 mF cm⁻²	3
CuSe@MnOOH	CuSe@FeOOH	PVA/LiCl	1.3 V	20.5 mF cm ⁻²	4
Ag@ppy	Ag@ppy	PVA/H ₃ PO ₄	0.8 V	47.5 mF cm⁻²	5
LIC-MOFs	LIC-MOFs	1M H ₂ SO ₄	1.0 V	8.1 mF cm ⁻²	6
MWCNTs	MWCNTs	PVA/H ₃ PO ₄	1.0 V	19.5 mF cm ⁻²	7
Ni@MnO ₂	Ni@MnO ₂	CMC/Na ₂ SO ₄	0.8 V	10.8 mF cm ⁻²	8
B-doped Graphene	B-doped Graphene	PVA/H ₂ SO ₄	1.0 V	16.5 mF cm ⁻²	9
Co(OH) ₂	VN	PVA/KOH	1.5 V	21.0 mF cm ⁻²	10
CuSe@Ni(OH) ₂	CuSe@Ni(OH) ₂	PVA/LiCl	1.0V	11.6 mF cm ⁻² (38.9 F cm ⁻³)	11
Ni-Co-P@LDHs	FeOOH	PVA/KOH	1.4 V	24.0 mF cm⁻²	Our Work

References:

1. Y. Li, H. Xie, J. Li, Y. Bando, Y. Yamauchi and J. Henzie, *Carbon*, 2019, **152**, 688-696.
2. C. Couly, M. Alhabeb, K. L. Van Aken, N. Kurra, L. Gomes, A. M. Navarro-Suarez, B. Anasori, H. N. Alshareef and Y. Gogotsi, *Advanced Electronic Materials*, 2018, **4**, 1700339
3. T. Cheng, Y. W. Wu, Y. L. Chen, Y. Z. Zhang, W. Y. Lai and W. Huang, *Small*, 2019, **15**, 1901830..
4. J. C. Li, J. F. Gong, X. S. Zhang, L. Z. Lu, F. Liu, Z. H. Dai, Q. J. Wang, X. H. Hong, H. Pang and M. Han, *ACS Applied Energy Materials*, 2020, **3**, 3692-3703.
5. L. Liu, Q. Lu, S. L. Yang, J. Guo, Q. Y. Tian, W. J. Yao, Z. H. Guo, V. A. L. Roy and W. Wu, *Advanced Materials Technologies*, 2018, **3**, 1700206.
6. W. Zhang, R. Li, H. Zheng, J. S. Bao, Y. J. Tang and K. Zhou, *Advanced Functional Materials*, 2021, **31**, 2009057.
7. B. B. Nie, X. M. Li, J. Y. Shao, C. M. Li, P. C. Sun, Y. C. Wang, H. M. Tian, C. H. Wang and X. L. Chen, *Nanoscale*, 2019, **11**, 19772-19782.
8. Y. B. Chen, S. J. Xie, G. J. Li, S. S. Jia, X. D. Gao and X. M. Li, *Applied Surface Science*, 2019, **494**, 29-36.
9. Z. W. Peng, R. Q. Ye, J. A. Mann, D. Zakhidov, Y. L. Li, P. R. Smalley, J. Lin and J. M. Tour, *ACS Nano*, 2015, **9**, 5868-5875.
10. S. Wang, Z. S. Wu, F. Zhou, X. Y. Shi, S. H. Zheng, J. Q. Qin, H. Xiao, C. L. Sun and X. H. Bao, *NPJ 2D Materials and Applications*, 2018, **2**, 7.
11. J. Gong, J.-C. Li, J. Yang, S. Zhao, Z. Yang, K. Zhang, J. Bao, H. Pang and M. Han, *ACS Applied Materials & Interfaces*, 2018, **10**, 38341-38349.